GRAY-TO-BLUE-TO-VIOLET HYDROGEN-RICH DIAMONDS FROM THE ARGYLE MINE, AUSTRALIA

Carolyn H. van der Bogert, Christopher P. Smith, Thomas Hainschwang, and Shane F. McClure

The Argyle diamond mine is the only known source of type IaB hydrogen- and nitrogen-rich diamonds colored gray to blue to violet. Twenty such diamonds were studied to investigate the relationships between their spectroscopic characteristics and color grades. The unusual color is the result of broad absorption bands centered at ~520–565 nm and 720–730 nm. A pronounced 551 nm band is superposed on the 520–565 nm feature. Spectral deconvolution of this feature suggests that it may be a composite, including H-related absorptions at ~545 and 563 nm and bands at 520–530 and 551 nm. The near- and mid-IR regions exhibit strong absorptions, including those related to H and N, many of which become more intense with increasing color saturation. The PL spectra exhibit peaks associated with nickel-related defects, which may play an important role in the coloration of the more violet diamonds in this group. H-rich gray-to-blue-to-violet diamonds, which are not known to be treated, can be readily separated from similar-hued diamonds that may be HPHT enhanced or synthetic.

Although a common impurity in type Ia diamonds, hydrogen is thought to influence the color of only a small proportion of them (Fritsch and Scarratt, 1992). These relatively H-rich diamonds fall into four color groups, as described by Fritsch et al. (1991, 2007a) and Fritsch and Scarratt (1992, 1993): (1) "brown to grayish yellow to green," (2) "white," (3) "chameleon," and (4) "gray to blue to violet." While H-rich brown and yellow diamonds are very common, gray-to-blue-to-violet diamonds are quite rare, particularly stones with high color saturation and those that are larger than half a carat (figure 1). Because these diamonds are characterized by their high H content and unusual color, this article will refer to them as "HGBV" (H-rich gray to blue to violet) diamonds.

The gemological characteristics of HGBV diamonds were first described by Fritsch and Scarratt (1989, 1992, 1993) and Fritsch et al. (1991), along with their dominant infrared (IR) and ultraviolet-visible (UV-Vis) spectral characteristics. The IR and UV-Vis characteristics were also reported in De Weerdt and Van Royen (2001). A recent study of thousands of small stones provided an updated view of these spectral characteristics for H-rich diamonds in general, including the HGBV color group (Fritsch et al., 2007a). All these studies showed that the IR spectra—of all the color groups of H-rich diamonds—are dominated by H-related peaks, and suggested that their UV-Vis spectra may be influenced by the relatively high H content. Photoluminescence (PL) optical characterization (Iakoubovskii and Adriaenssens, 2002) and electron paramagnetic resonance (EPR) measurements (Noble et al., 1998) of HGBV diamonds have been performed as well; these studies revealed nickel defects that may also influence their color.

The present article describes gemological observations and a focused spectroscopic (UV-Vis, IR, and PL) and DiamondView imaging study of 20 HGBV diamonds. We describe how these data characterize

Figure 1. Two of the largest HGBV diamonds faceted to date are set in the yellow metal rings shown here—a 2.34 ct Fancy Dark violet-gray emerald cut and a 1.06 ct Fancy Dark gray-blue oval—and were included in this study. The ring on the upper right is a striking combination of Argyle diamonds, with a 1.38 ct Fancy red center stone, flanked by gray-violet and near-colorless diamonds. The loose 0.73 ct pear-shape, also part of this study, is Fancy Deep grayish violet. The yellow metal rings were designed and manufactured by Jean Mahie; the other items were provided by L. J. West Diamonds. Photo by Robert Weldon.

the material and relate to its GIA color grades. In particular, we investigated the different UV-Vis-NIR spectra of violet- as compared to blue-hued samples through analysis of their two major absorption minima, which affect their apparent color (e.g., Fritsch et al., 2007a). In addition, we performed Gaussian modeling of the major 520–565 nm absorption feature to explore whether it is composed of several individual bands (i.e., a composite), as suggested by Fritsch et al. (1991).

SOURCE OF HGBV DIAMONDS: THE ARGYLE MINE

The Argyle mine in northwestern Australia (see, e.g., Shigley et al., 2001) is the source of H-rich diamonds from at least two different color groups: brown to grayish yellow to green (Fritsch and Scarratt, 1993; Massi, 2006; Fritsch et al., 2007a), and gray to blue to violet (Fritsch and Scarratt, 1992, 1993; Noble et al., 1998; Iakoubovskii and Adriaenssens, 2002). Argyle is currently the only known source of HGBV diamonds, which represent a minute proportion of the mine's output. The rough typically occurs as irregular fragments, most of which are fashioned as melee ranging from a few points to about 0.20 ct. Much of this material has an unremarkable, unsaturated color.

Some larger pieces of rough with more saturated color are encountered, but faceted stones over half a

carat are very rare, and only a few weighing more than one carat have been recovered in the 25+ years since mining began at Argyle. When available, the finest stones of this color variety have been sold through the yearly Argyle pink diamond tender. For example, two of the 63 stones offered at the 2006 tender were HGBV diamonds, a proportion that approximately reflects the relative production of tender-quality HGBVs to pinks at the mine (Max, 2006). Between 1993 and 2008, a total of 20 HGBV diamonds, ranging from 0.39 to 2.34 ct, were offered at the tender (Argyle Diamonds, 1993–2008; see *G&G* Data Depository at www.gia.edu/gemsandgemology). The 2.34 ct stone was a Fancy Dark violet-gray emerald cut (again, see figure 1). In spring 2009, Rio Tinto will offer its first exclusive tender of blue and violet diamonds, representing select material from several years of production (Rio Tinto, 2009).

MATERIALS AND METHODS

Samples. During the course of this research, more than 30 HGBV diamonds passed through the GIA Laboratory in New York for origin-of-color determination and grading services. Of these, 18 representative stones were selected for study (see table 1 and, e.g., figure 2). In addition, two exceptional stones set in yellow metal rings were loaned to the laboratory (again, see figure 1); both had received GIA Colored Diamond grading reports prior to being set. All 20 of

the samples were reportedly from the Argyle mine; they had Argyle inscriptions or were submitted by Rio Tinto NV (or both). Several were also offered at various Argyle pink diamond tenders.

Some spectroscopic measurements could not be made on all the diamonds in this group because of time constraints. In addition, some samples were not suited to certain spectroscopic measurements due to interference from their jewelry settings or the cut geometry of the stone. However, all the samples were examined using other standard gemological tests (see below).

Grading and Testing Methods. GIA color grades were determined by experienced graders using the standard conditions and methodology of GIA's colored diamond grading system (King et al., 1994). Internal features were observed with a standard binocular microscope using a variety of lighting techniques and magnification up to 100×. Most of the stones received Colored Diamond Identification and Origin Reports, which do not include clarity

grades, so any discussion of clarity characteristics is unrelated to specific clarity grades. Reaction to UV radiation was observed in a darkened room with a conventional 4-watt combination long-wave (365 nm) and short-wave (254 nm) UV lamp. All the unmounted stones were also examined with a De Beers Diamond Trading Co. DiamondView deep-UV (<230 nm) luminescence imaging system (Welbourn et al., 1996). We used a handheld spectroscope to view absorption features in the visible range, with the stones both at room temperature and after immersion in liquid nitrogen (~77 K). We checked for electrical conductivity by putting the diamond on a metal plate and touching it in several places with an electrical probe.

Most of the samples were analyzed by a variety of spectroscopic techniques. For 15 diamonds, we recorded absorption spectra in the UV-Vis-NIR region (250–850 nm) using a Thermo-Spectronic Unicam UV500 spectrophotometer with a sampling interval of 0.1 nm and a spectral bandwidth of 0.5 nm. The samples were mounted in a cryogenic cell and cooled with liquid nitrogen. Because the path lengths of the light through the faceted stones were not known, it was impossible to normalize the UV-Vis-NIR data so the individual samples could be directly compared. However, we were able to compare ratios of areas and heights calculated for each individual spectrum (e.g., Gaffey et al., 1993).

Absorption spectra in the mid-IR (6000–400 cm^{-1}; 1 cm^{-1} resolution) and near-IR (11000–2700 cm^{-1}; 4 cm^{-1} resolution) regions were recorded for 12 diamonds at room temperature with a Thermo-Nicolet Nexus 6700 Fourier-transform infrared (FTIR) spectrometer, equipped with KBr and quartz beam splitters. A 6× beam condenser focused the incident beam on the sample, and 1,024 scans per spectrum were collected to improve the signal-to-noise ratio. Since true normalization was not possible, we scaled the data at 2700 cm^{-1} in the three-phonon region to compare the amplitudes of the IR peaks between stones of different color grades.

Low-temperature PL spectra were collected on 10 stones using a Renishaw 1000 Raman microspectrometer at three different laser excitations. We used 50-milliwatt Ar-ion lasers for two different laser excitations: 488.0 nm for the 490–850 nm range and 514.5 nm for the 517–850 nm range. A He/Ne laser produced a 632.8 nm excitation for the 640–850 or 690–850 nm range. The samples were cooled by direct immersion in liquid nitrogen. Three scans were collected for each measurement to improve the

TABLE 1. The 20 HGBV diamonds examined for this study, listed from bluest to grayest to most violet.

GIA color grade[a]	Weight (ct)	Shape	Spectra collected
FDK gray-blue[b]	1.06	Oval	—
FDK gray-blue	1.02	Shield	UV-Vis-NIR; IR; PL
FDK gray-blue[c]	0.23	Marquise	UV-Vis-NIR
FAN gray-blue	0.51	Pear	UV-Vis-NIR; IR; PL
FAN gray-blue[c]	0.24	Cushion	—
FAN gray-blue	0.21	Pear	UV-Vis-NIR; IR; PL
FAN gray-blue[c]	0.23	Round	UV-Vis-NIR; PL
FAN grayish blue[c]	0.22	Modified heart	—
FDK gray[c]	1.57	Cushion	IR
FAN violet-gray[c]	0.15	Round	UV-Vis-NIR
FDK violet-gray[b]	2.34	Emerald	—
FAN gray-violet	0.26	Cushion	UV-Vis-NIR; IR; PL
FDK gray-violet	0.56	Modified oval	UV-Vis-NIR; IR; PL
FDK gray-violet[c]	0.25	Pear	UV-Vis-NIR; PL
FAN grayish violet	0.16	Round	UV-Vis-NIR; IR; PL
FAN grayish violet[c]	0.09	Round	UV-Vis-NIR; IR
FDP grayish violet	0.52	Cushion	UV-Vis-NIR; IR; PL
FDP grayish violet	0.65	Oval	UV-Vis-NIR; IR; PL
FDP grayish violet	0.73	Pear	UV-Vis-NIR; IR; PL
FDP grayish violet[c]	0.10	Round	UV-Vis-NIR; IR

[a]FDK = Fancy Dark, FAN = Fancy, FDP = Fancy Deep
[b]These diamonds were set in rings, which prevented the collection of some spectroscopic data.
[c]Complete data sets for these stones could not be collected due to time constraints and/or unfavorable conditions caused by cut geometry.

Figure 2. These are three of the HGBV diamonds examined for this study: a 0.65 ct Fancy Deep grayish violet oval, a 0.56 ct Fancy Dark gray-violet modified oval, and a 1.02 ct Fancy Dark gray-blue shield cut. Photos by C. H. van der Bogert.

signal-to-noise ratio. For the general PL measurements, the laser was slightly defocused to collect a bulk measurement. In addition, focused measurements of one sample were taken at the 488.0 nm excitation to investigate differently fluorescing regions. All the spectra were scaled to the diamond Raman peaks, so the amplitudes of the absorption features could be compared.

Gaussian Modeling. Fritsch et al. (1991) suggested that a broad band observed in HGBV diamonds at 520–565 nm was a composite of multiple absorption bands. To test this theory, we performed basic spectral deconvolutions for 10 of the highest-quality UV-Vis-NIR spectra using Origin analytical software (www.originlab.com) to identify the major absorption bands contributing to the composite feature. Individual absorption bands were generally assumed to have a Gaussian (bell curve) shape, and composite absorption bands were considered the sum of multiple individual Gaussian curves, termed *Gaussian components* (e.g., Burns, 1993). The Gaussian components were modeled by spectral deconvolution, which determines the component positions and widths that best reproduce a composite absorption band, such as the one seen in HGBV diamonds (figure 3). The modeling technique requires the establishment of a baseline from which the calculations are made. This study used a straight baseline defined by the absorption minima that bounded the proposed composite feature.

RESULTS AND ANALYSIS

Color Appearance. The HGBV diamonds in this study were found to have natural color within a limited range of fancy grades (table 1): Fancy, Fancy Deep, and Fancy Dark. None of the samples had fancy grades

with lighter tone—Fancy Light, Very Light, Light, or Faint—or with higher saturation and moderate tone—Fancy Intense or Fancy Vivid. Thus, the samples had relatively low saturation and dark tone. When saturation is very low, a hue modifier is assigned, because the stone appears brownish or grayish (King et al., 1994). All the blue and violet samples had gray modifiers—gray-blue, grayish blue, gray-violet, and grayish violet. Some samples were primarily gray with blue or violet modifiers—bluish gray and violet-gray (table 1).

Figure 3. Spectral deconvolution of the 520–565 nm broad band using Gaussian components suggests that it is a composite of multiple absorption bands. The peak positions were modeled using a baseline defined by the minima on each side of the composite band.
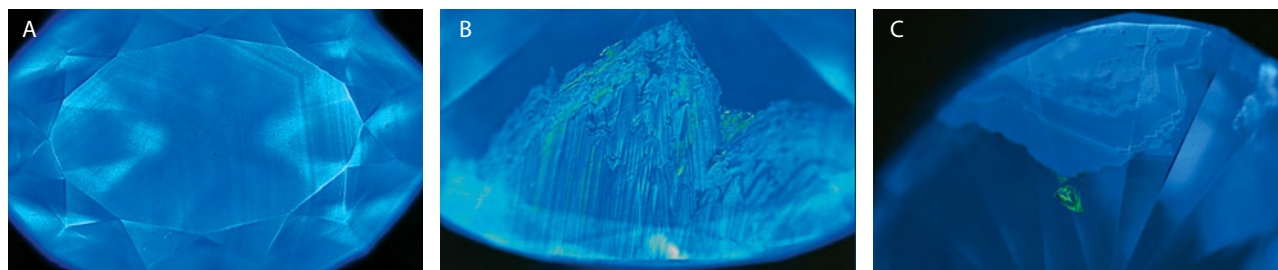

SPECTRAL DECONVOLUTION
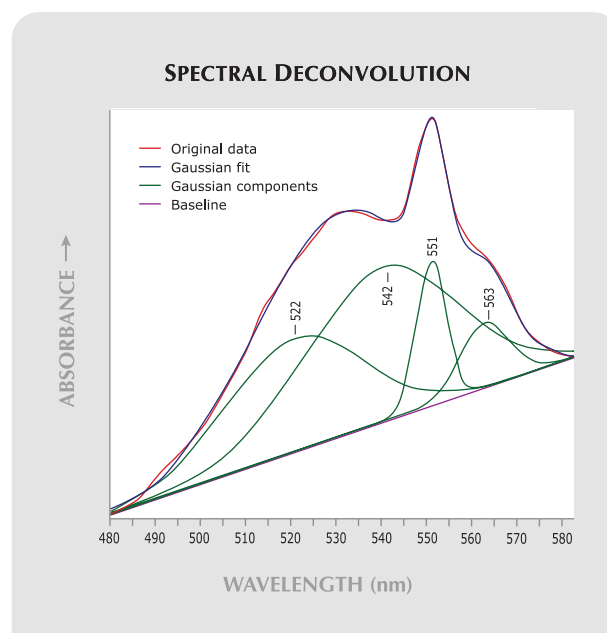
Figure 4. Many of the diamonds displayed subtle blue fluorescence zoning when examined with the DiamondView (A, magnified 20×). However, half the stones contained discrete zoned areas with alternating intensities of brighter blue fluorescence, sometimes with very thin yellowish green fluorescent layers (B, magnified 30×) and/or isolated yellowish green fluorescing regions (C, magnified 40×). Photomicrographs by C. H. van der Bogert.

One of the samples had such low saturation that it was impossible to discern a specific hue, so it was classified as gray (again, see table 1). None of the samples exhibited bluish violet or violetish blue hues.

Ultraviolet Fluorescence and Phosphorescence. All the diamonds in this study had consistent fluorescence reactions. When exposed to long-wave UV radiation, each exhibited a slightly chalky yellow reaction of moderate-to-strong intensity. Exposure to short-wave UV produced a weak-to-moderate reaction of the same color. However, samples with weaker saturation (i.e., those that appeared grayer) tended to phosphoresce weak-to-strong yellow to both long- and short-wave UV, while those that were relatively stronger in saturation did not phosphoresce.

DiamondView Imaging. The samples showed a variety of reactions when examined with the DiamondView. Typically, they fluoresced medium blue with subtle alternating brighter and darker blue planar and angular zones (figure 4A). Ten of the 18 unmounted samples exhibited discrete areas of brighter and darker blue layers alternating with very thin yellowish green layers conforming to cubo-octahedral growth zones (figure 4B). Occasionally, yellowish green fluorescence was present in small isolated zones (figure 4C); though such zones were found in samples of all color grades, they tended to be larger and brighter in violet-hued stones. The differences between the blue and yellowish green areas were further investigated with focused PL analyses (see below).

Electrical Conductivity. None of the samples in this study were electrically conductive.

Microscopic Characteristics. *Inclusions.* In general, the HGBV diamonds contained only a limited range of inclusions, compared to the wider range seen in diamonds overall. Most common were etch features (including etch channels), tubes, acicular cavities, and pits. The etch channels occurred along cleavage directions and were quite deep in some cases (figure

Figure 5. HGBV diamonds exhibited different types of characteristic internal features. These included (left, magnified 52×) coarsely textured channels, where chemical etching occurred along preexisting cracks or cleavages; they can sometimes be very deep, as seen in the 0.73 ct stone in the center (magnified 40×). Another type of feature (right, magnified 52×), either etch or growth tubes, consists of hollow, icicle-like acicular inclusions. Photomicrographs by C. P. Smith.
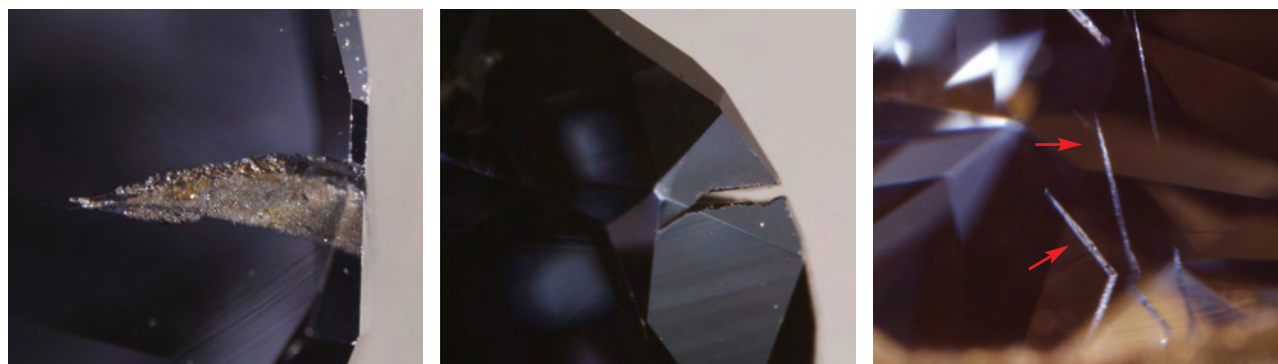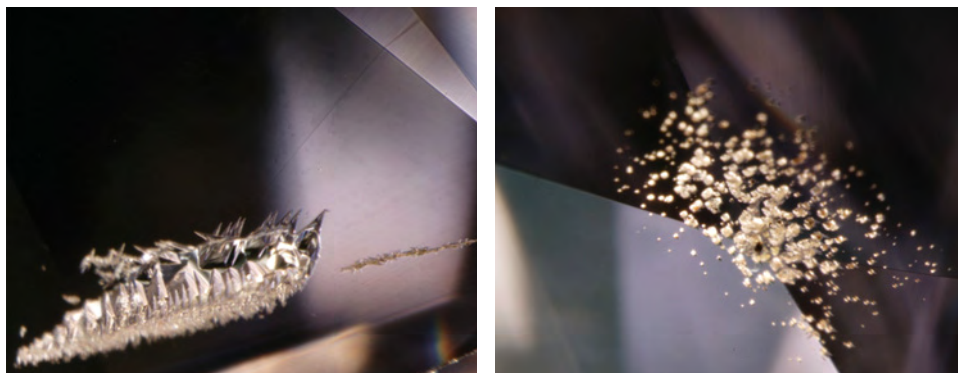
Figure 6. Also present in the HGBV diamonds were shallow cavities that resembled furrows with radiating acicular margins (left) and fields of small pits (right), which may be either etch features or remnants of inclusions removed during cutting. Photomicrographs by C. H. van der Bogert; magnified 40×.

5). Long, icicle-like tubes (figure 5, right), cavities with clusters with radiating acicular margins (figure 6, left), and small pointy pits (figure 6, right) were also seen in many of the samples. All these features occurred singly or as tight clusters and all were surface-reaching. The small pits appeared to be the remnants of larger features that were removed during cutting.

Only two of the 20 samples contained large "crystal" inclusions. These were colorless (possibly negative) crystals and black to dark brown acicular crystals, all of which were inert in the Diamond-View (figure 7) and could not be identified with the analytical techniques available. We observed graphitized stress fractures in two other samples. Pinpoints and clouds were seen in most of the samples, sometimes present as wisp-like patterns or stringers.

Internal Growth Structures, Color Zoning, and Strain. Viewed through an optical microscope, color zoning typically occurred as subtle zones with higher saturation (darker gray, or more blue or violet) than the surrounding areas (figures 7, left, and 8). The zones typically had either straight or slightly wavy planar boundaries. Occasionally, rectangular planar brownish zones or sectors were observed. A few samples exhibited surface grain lines that were frequently associated with the color zoning. Obvious internal growth structures were generally absent, though turbidity along some of the growth structures was sometimes seen both in transmitted light and with the DiamondView imaging system. The areas with stronger coloration had a weaker blue luminescence than the weakly colored areas (figure 7). In transmitted light, the green fluorescent areas observed with the DiamondView were not noticeably different from the weaker blue fluorescent areas.

The stones showed weak strain following the cubo-octahedral growth planes when observed using crossed polarizers with transmitted light (figure 9).

UV-Vis-NIR Spectroscopy. *Observations of Spectra.* When we viewed the HGBV diamonds with a standard desk-model spectroscope, typically only a weak-to-moderate broad band at approximately 550 nm was observed, though occasionally a weak band at 594 nm was noted. Stones with more dominant gray color also exhibited a weak line at 415 nm.

The dominant absorptions in the spectrophotometer data were a series of broad bands centered at 520–565 nm, 720–730 nm, ~760 nm, and ~835 nm (figure 10). The 520–565 nm feature extended from approximately 460 to 600 nm, with a typical maximum at 530–550 nm. It was superposed by a narrower band centered at 551 nm, typically extending from 545 to 560 nm at the base. While the centers of all the broad absorption features varied within the study group, the 551 nm peak did not.

Figure 7. Mineral inclusions were uncommon in the HGBV diamonds. When present, they were primarily clusters of radiating dark brown to black acicular crystals (left), with a form similar to those of some etch features. The planar, slightly wavy color zoning adjacent to the inclusion was also seen with the DiamondView (right). Areas with stronger violet coloration had weaker blue fluorescence than areas with less violet coloration. Major color zoning is marked with arrows. Photomicrographs by C. H. van der Bogert; magnified 40×.
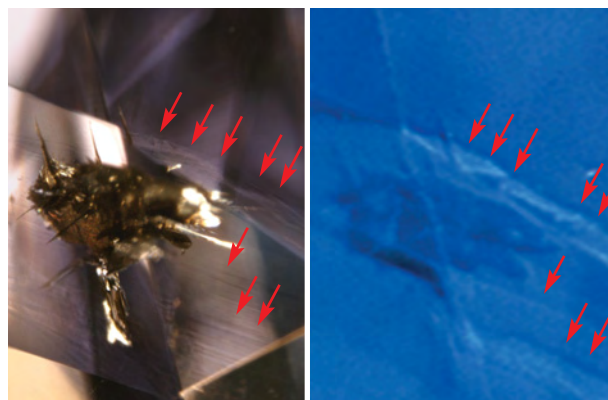
Figure 8. Subtle color zoning in many of the diamonds typically consisted of more-saturated violet zones adjacent to less-saturated and occasionally brownish zones, which followed indistinct growth structures or occurred in sectors. Photomicrographs by T. Hainschwang (left, in immersion) and C. H. van der Bogert (right, diffused light); magnified 20×.

Many weaker peaks and broad bands were also seen in the UV-Vis range (again, see figure 10). There was a general increase in absorption into the UV, with a subtle broad feature centered at 350 nm. Other weak peaks included a 379/380 doublet and individual peaks at 405, 415 (N3 zero-phonon line), 425, 445, and 448 nm. Commonly, a weak composite band centered at 594 nm, roughly 10 nm wide, was present. In addition, the strongly saturated samples exhibited very weak peaks at 603, 608, 610, 618, and 630 nm.

Spectral Analysis. Variations between the violet- and blue-hued samples were evaluated by comparing different aspects of their spectra (figure 11A). First, we investigated the center positions of the two broad

absorption minima in the blue (B_{min}) and red (R_{min}) regions. These positions were found to vary with hue. Samples with violet hues had absorption mini-

Figure 10. The UV-Vis-NIR spectra of HGBV diamonds are characterized by a strong broad band at 520–565 nm, with a smaller superposed 551 nm broad band, a second strong broad band centered at 720–730 nm, and two smaller broad bands at ~760 and ~835 nm. The position of the 551 nm band did not vary, but the positions of the other broad bands varied slightly with color grade. The spectra were collected at ~77 K and are offset vertically for clarity. FAN = Fancy, FDK = Fancy Dark, and FDP = Fancy Deep.

Figure 9. A low degree of internal strain was characteristic of the HGBV diamonds, which exhibited only subtle gray and blue interference colors, with angular streakiness characteristic of cubo-octahedral growth. This is in contrast to the banded and tatami-patterned strain characteristic of type IIb blue and type IIa pink diamonds, and the high degree of mottled strain typical of type Ia pink-to-purple diamonds. Photomicrograph by T. Hainschwang; magnified 20×.
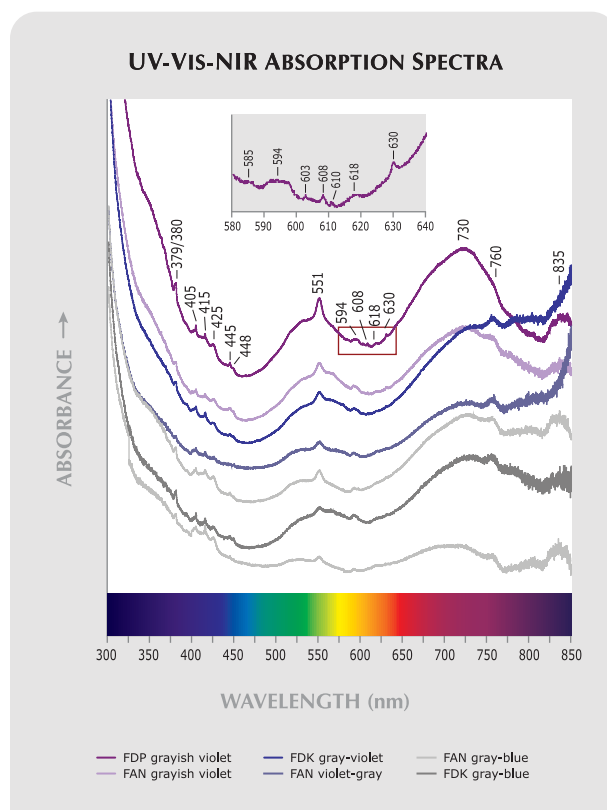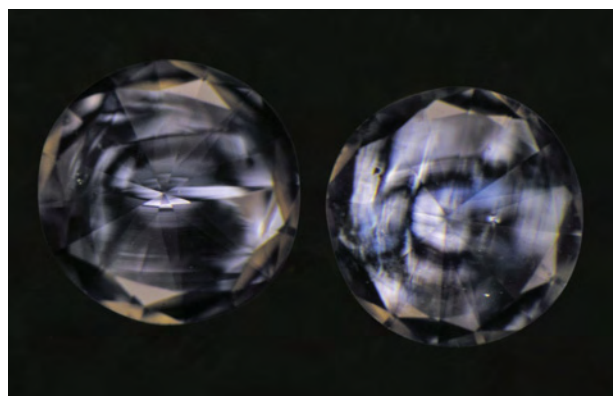
ma at 455–467 nm in the blue region and 601–613 nm in the red, whereas samples with blue hues had minima at higher wavelengths (460–490 nm) in the blue and lower wavelengths (568–602 nm) in the red (figure 11B). On average, the positions of the minima were 127 nm apart for the violet-hued samples, and 108 nm apart for the blue-hued samples.

Next, we compared the relative strengths (i.e., the areas; see figure 11A) and depths (figure 11C) of the absorption minima in the blue and red regions. We calculated the ratio of the area of the blue absorption minimum (B_a) between 380 and 551 nm to the area of the red absorption minimum (R_a) between 551 and 720 nm, and the ratio of the depth of the blue absorption minimum (B_d) to the depth of the red absorption minimum (R_d). Most of the samples with blue hues had B_a/R_a (1.9–2.1) and B_d/R_d (1.5–1.7)—higher than those with violet hues. The violet-hued samples had B_a/R_a of 1.4–1.7 and B_d/R_d of 1.3–1.5 (figure 11C).

Gaussian Modeling. Each of the 10 UV-Vis-NIR spectra was modeled in two different ways to explore the possibility that the 520–565 nm absorption was a composite of multiple bands. First, we allowed the software to automatically calculate peak positions based on three to four starting positions. For example, the starting positions selected for the composite feature in figure 3 were 522, 542, 551, and 563 nm, based on the inflection points at the last three positions and the large width of the feature toward the UV. Our software allowed the peak positions and widths to vary without constraint in order to maximize the fit of the Gaussian components to the composite feature. A model was considered successful when multiple model runs using a variety of starting positions resulted in reasonable positive peak heights and areas, as well as similar final peak positions for each modeling attempt, and when R^2 (a measure of how well the model fits the spectrum) was 0.99 or greater. The goal was to achieve the best statistical fit of the composite feature while using as few peaks as possible. While models with more than three or four peaks could yield improved R^2 values, the additional peaks would represent a statistically insignificant proportion—less than 1%—of the overall composite feature.

Using this approach, we found that the 520–565 nm absorption in most of the samples was a composite feature, best modeled as a combination of four independent absorption peaks centered at 520–530 nm (with an average value of 527 nm),

ANALYSIS OF UV-VIS ABSORPTION SPECTRA

POSITION OF MINIMA IN RED AND BLUE REGIONS
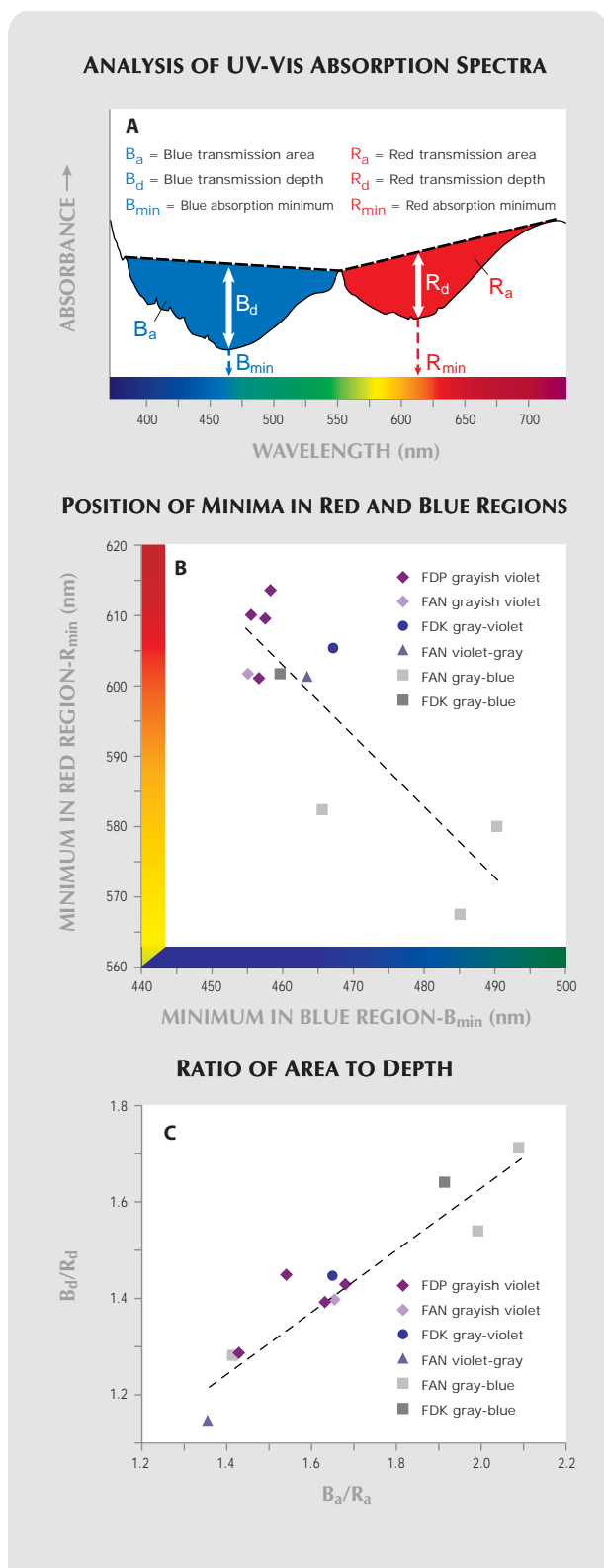
RATIO OF AREA TO DEPTH

Figure 11. The spectral differences between the samples were investigated by comparing the positions of the absorption minima of the major transmission windows in the blue and red regions (A and B), and the ratios of the areas of these windows to their depths (A and C).
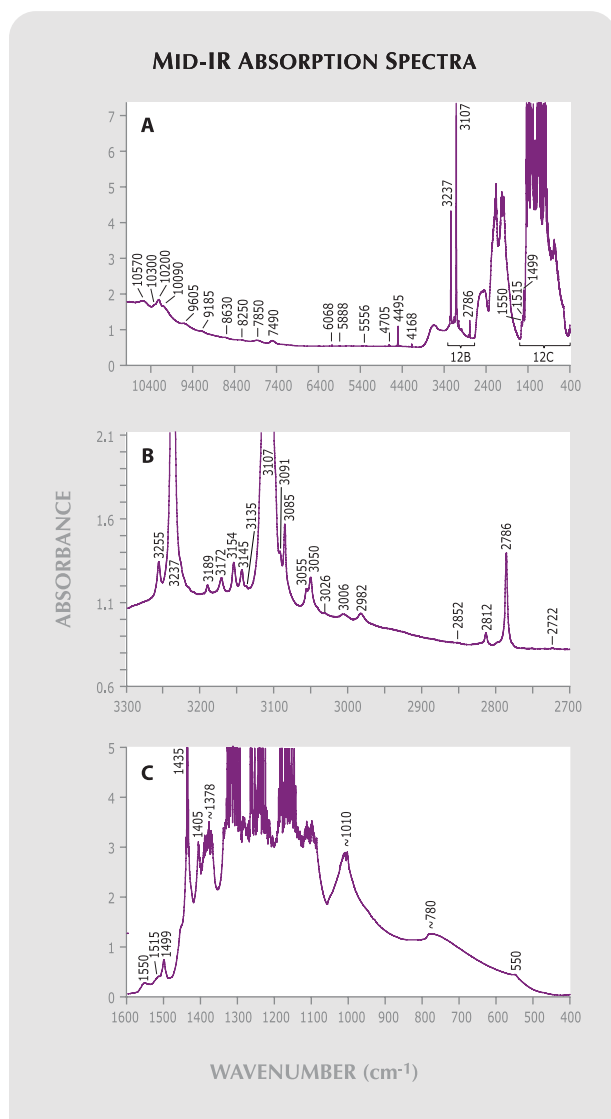
MID-IR ABSORPTION SPECTRA

Figure 12. A strongly colored (Fancy Deep) grayish violet diamond had the most intense absorption peaks across all measured regions as shown in this composite spectrum (A). The peaks were seen in other HGBV diamonds, but with lower intensity. HGBV diamonds are characterized by multiple sharp, strong, hydrogen-related peaks. These include the 3107 cm^{-1} peak and its associated peaks at 6068, 5888, 5556, and 4495 cm^{-1}, as well as those at 3237 and 2786 cm^{-1}. Numerous other small peaks observed throughout the mid- to near-IR region (B) were characteristic of all the diamonds in this study (see also figure 13). It was possible to identify these diamonds as type IaB and, in some cases, to calculate the concentration of IR-active nitrogen (C).

543–549 nm (average 546 nm), 551 nm (without variation), and 557–566 nm (average 563 nm). For some samples, however, the models were not consistently reproducible using four peaks; the final

position of the 543–549 nm peak varied widely. For these spectra, reproducible model fits were possible only by using three peaks: 526–530 nm (average 529 nm), 551 nm (without variation), and 556–572 nm (average 563 nm).

Then, based on these results, we tested the hypothesis that the composite feature consists of a 551 nm peak plus two hydrogen-related peaks—545 and 563 nm—seen in other colors of H-rich diamonds. For these model runs, we constrained the position of the 545, 551, and 563 nm peaks to test whether valid models could be fit to the spectra under these conditions. For all 10 spectra, we were able to fit the composite feature with peaks at 545, 551, and 563 nm if a fourth peak in the region 520–528 nm was allowed to be present. The position of the fourth peak was not constrained. For these models, R^2 ranged between 0.987 and 0.998, indicating that these peaks are reasonably good fits to the composite feature. It should be kept in mind, however, that these models do not represent unique solutions.

Infrared Spectroscopy. All the diamonds proved to be type IaB, with a very high concentration of hydrogen (Woods and Collins, 1983; e.g., figure 12). Although total absorption in the one-phonon region was common, for five samples (e.g., figure 12C) it was possible to use spectral fitting techniques (Kiflawi et al., 1994; Boyd et al., 1995) to determine that the concentration of IR-active nitrogen ranged from 1350 to 2700 ppm. We observed a platelet peak extending from 1376 to 1368 cm^{-1}, seen in another study of Argyle diamonds (Noble et al., 1998), in only a few samples. We typically recorded bands at ~1550, 1515, and 1499 cm^{-1} (figure 12A); in some samples, peaks at 1435, 1405 cm^{-1} were also present, along with broad features at ~1010, 780, and 550 cm^{-1} (figure 12C).

After the IR absorptions associated with nitrogen, the most significant were those related to hydrogen (e.g., Woods and Collins, 1983; Fritsch and Scarratt, 1989; Fritsch et al., 1991). A series of sharp peaks were recorded between 3300 and 2700 cm^{-1}, with two dominant peaks at 3237 and 3107 cm^{-1} (figures 12B and 13A,B). Several other weaker bands were recorded between 4705 and 4168 cm^{-1} (figures 12A and 13C). Very weak bands at 4678, 4412, 4236, and 4224 cm^{-1} were sometimes present. Weak, sharp bands were observed at 6068, 5888, and 5556 cm^{-1} (figure 12). Another series of broad absorption bands were positioned at 10570 cm^{-1} (946 nm), 10300 cm^{-1} (970 nm), 10200 cm^{-1} (980
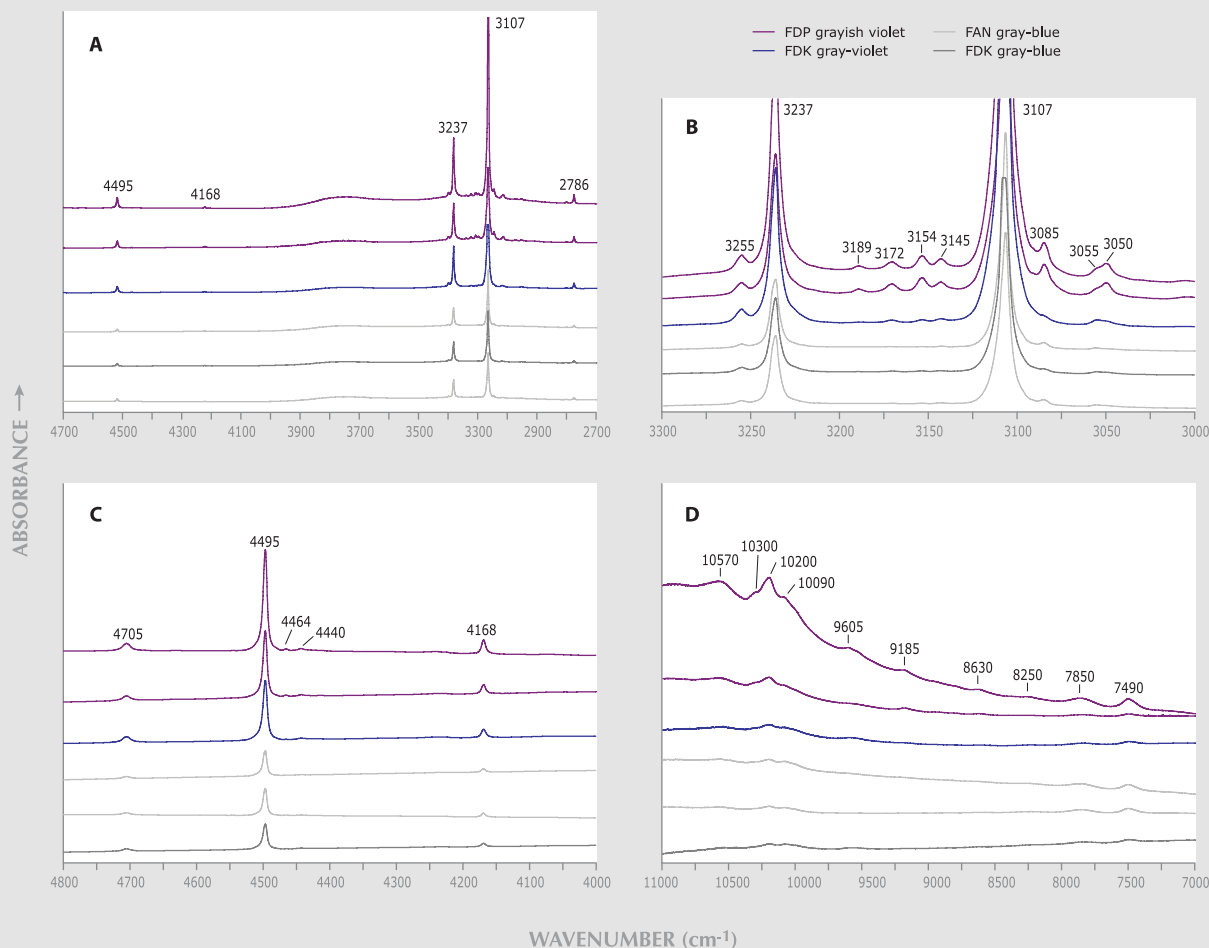
Figure 13. *Across the IR spectrum, the strength of the IR peaks and broad bands correlated with color. The violet-hued stones had stronger IR absorptions than the blue-hued stones for peaks between 4800 and 2700 cm⁻¹ that have been attributed to hydrogen (A, B, C). Broad peaks of unknown origin between 10570 and 8250 cm⁻¹ were also stronger in violet-hued stones, but the strengths of those at 7850 and 7490 cm⁻¹ did not seem to depend on color (D). The spectra were scaled at 2700 cm⁻¹ and are offset vertically for clarity.*

nm), 10090 cm⁻¹ (991 nm), and between 8630 and 7490 cm⁻¹ (figures 12 and 13D).

When we compared the IR peaks of stones with different color grades, we found that the strengths of these peaks generally depended on diamond hue. The 3107 cm⁻¹, associated 2786 cm⁻¹, and 3237 cm⁻¹ peaks were more intense in violet- than in blue-hued diamonds (figure 13A). The same relationship between peak intensity and hue also was seen for the weaker peaks in the regions 3300–3000 cm⁻¹ (figure 13B) and 4800–4000 cm⁻¹ (figure 13C), as well as for the 6068 and 5888 cm⁻¹ peaks. The strongest broad peaks between 11000 and 8000 cm⁻¹ were recorded in Fancy Deep grayish violet stones

(figure 13D). However, except for one such grayish violet diamond with very strong absorption, the Fancy gray-blue stones exhibited stronger absorptions at 7850 and 7490 cm⁻¹ than the diamonds with other color grades.

Photoluminescence Spectroscopy. As noted above, we used three different laser excitations to investigate the PL properties of the samples. Many PL centers were activated by different excitations to varying degrees, while others were only active for specific excitations (figure 14). All the spectra were scaled to the Raman peaks, so we could compare the amplitudes of the absorption features.
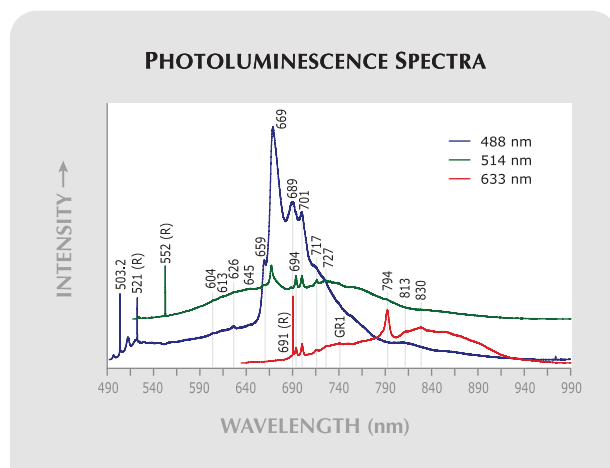
PHOTOLUMINESCENCE SPECTRA

Figure 14. These spectra, typical for HGBV diamonds, were collected for a Fancy Deep grayish violet diamond cooled to ~77 K at three excitation wavelengths (488, 514, and 633 nm). The 488 nm excitation caused strong luminescence in the 650–750 nm region, with dominant PL bands at 669, 689, and 701 nm, and weaker bands at 659 and 717 nm. Weak broad peaks were present at 503.2 (H3), 604, 613, 626, and 645 nm. The 514 nm excitation exhibited strong peaks at 669 and 701 nm, but it also showed distinct peaks at 694 and 717 nm. A 794 nm (NE8) peak was strongest under 633 nm excitation. The spectra were scaled to the Raman peaks (R) and offset vertically for clarity.

488 nm Excitation. With 488 nm excitation, the dominant luminescence consisted of a series of strong broad bands between ~650 and 750 nm (figures 14 and 15A). These included strong peaks at 669, 689, and 701 nm, with weaker bands at 659 and 717 nm. The asymmetries of some of these features suggest they are composite bands. In particular, the 689 nm peak likely includes a 694 nm luminescence, as observed with the 514 nm excitation (see below).

A weak 604 nm peak was often present with its associated vibronic system at 613 and 626 nm, as described by Iakoubovskii and Adriaenssens (2002). Some stones had weak broad bands positioned at 496, 504, and 512 nm—the higher-energy phonon replicas of the S2 (NE1) zero-phonon line at 489.2 nm, which itself could not be observed because of its proximity to the laser line. Seen in natural type IaB diamonds, the NE1 is associated with nickel-vacancy complex defects (Nadolinny and Yelisseyev, 1994).

Two stones exhibited a 496.7 (S3; Zaitsev, 2001) nm band, which is associated with mixed-habit cubo-octahedral growth. Some of the spectra also exhibited peaks at 503.2 nm (figure 14) or at 502.8 and 503.2 nm (figure 15A, inset). The 503.2 nm peak is seen in nitrogen-containing diamonds (H3;
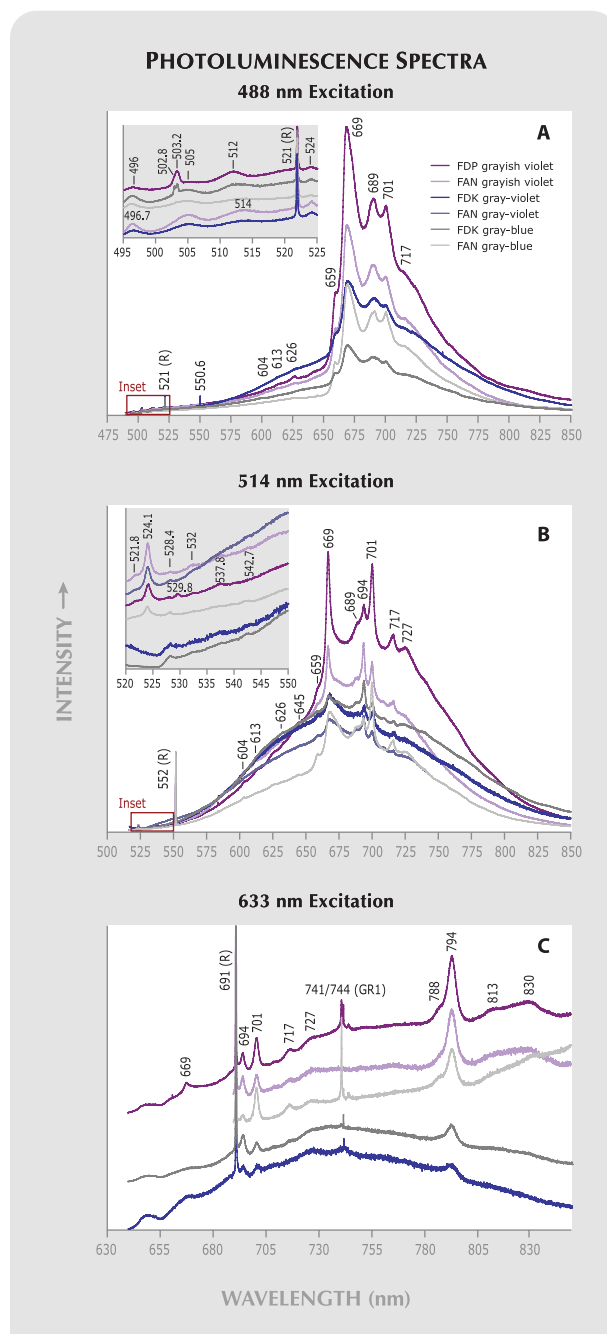

Figure 15. PL spectra were collected for different colors of HGBV diamonds cooled to ~77 K using three excitation wavelengths: (A) 488 nm, (B) 514 nm, and (C) 633 nm. The spectra were scaled to the Raman peaks (R), and the insets and (C) are offset vertically for clarity.

Zaitsev, 2001). Most of the spectra had a small broad peak centered at 524 nm. The violet-hued stones exhibited a 550.6 nm peak, which corresponds to the 551 nm peak seen in the UV-Vis-NIR spectra (figure 15A). A 746.8 nm peak, observed in the Fancy Dark gray-violet stone, is thought to be

associated with Ni (Yelisseyev and Kanda, 2007).

The major luminescence peaks (669, 689, and 701 nm) were stronger for violet-hued diamonds, and their intensity increased with color saturation (figure 15A). The 604 nm system was active only in the stones with the most violet color, those graded grayish violet. The 604, 659, 669, and 701 nm centers have been attributed to Ni defects (Bokii et al., 1986; Iakoubovskii and Adriaenssens, 2002), while the 645, 689, and 694 nm peaks are tentatively attributed to Ni defects (Iakoubovskii and Adriaenssens, 2002). The strengths of the peaks between 496 and 524 nm do not seem to have a direct relationship to hue or saturation.

514 nm Excitation. Many of the same features seen with 488 nm excitation were also present under 514 nm excitation, but they had slightly different characteristics (figures 14 and 15B). The dominant peaks again included those at 669 and 701 nm. The composite structure of the 689 nm peak became apparent as the 689 and 694 nm peaks resolved into a pair of peaks. In addition to the 659 and 717 nm bands on the flanks of the strongest luminescence peaks, there was a weak peak at 727 nm. The 717 and 727 nm peaks are phonon sidebands associated with the 701 nm vibronic system (Iakoubovskii and Adriaenssens, 2002).

The 604 nm system was also present at this excitation, in addition to a weak peak at 645 nm, both of which were stronger in the violet-hued stones. Some of the samples exhibited small peaks at 524.1 nm and weak bands at 521.8, 528.4, 532, 537.8, and 542.7 nm (figure 15B, inset). The most violet of these stones also showed a 529.8 nm peak. Two of the samples only exhibited small peaks at 528.4 and 542.7 nm. All had a 584.4 nm peak, the strength of which was greater in the violet-hued stones. As in the 488 nm excitation, the overall strength of the dominant peaks was strongest in the stones with the most saturated violet color.

633 nm Excitation. With this excitation, the 794 nm (NE8) peak was dominant (figures 14 and 15C). Additional peaks were present at 694, 701, 717, and 727 nm. The 669 nm peak appeared below the Raman peak in some cases. Many of the stones exhibited a GR1 zero-phonon line (741/744 doublet), which indicates radiation damage—in this case, natural radiation damage, because the stones were not treated in any way.

For this excitation, the relationship to color is less clear (figure 15C). However, the two stones with the strongest 794 nm peaks were both grayish violet. The gray-blue stones, however, had stronger luminescence peaks than the Fancy Dark gray-violet stone. Some stones with more saturated violet color also exhibited broad weak peaks at 788, 813, and 830 nm. The 813 and 830 nm features are associated with the zero-phonon line at 794 nm (Iakoubovskii and Adriaenssens, 2002). The 788 and 794 nm centers have been attributed to Ni defects (Bokii et al., 1986; Iakoubovskii and Adriaenssens, 2002).

488 nm Excitation Spot Analyses. We also investigated the PL differences between the yellowish green and blue fluorescing regions seen with the DiamondView (figure 4C) in a Fancy Deep grayish violet stone using the 488 nm excitation. We collected PL spectra from three focused areas: a yellowish green spot, a weak-to-moderate blue spot, and a stronger bright blue spot (figure 16). The bright blue spot corresponded to a region of less saturated color in the sample, while the yellowish green and weak-to-moderate blue fluorescing areas correlated with more saturated violet color. The yellowish green spot exhibited the strongest photoluminescence.

Figure 16. PL spectra for three areas with differently colored ultra short-wave UV fluorescence were collected from a Fancy Deep grayish violet diamond using an excitation wavelength of 488 nm. Areas with yellowish green fluorescence exhibited stronger Ni-related peaks than those with blue fluorescence. The spectra were scaled to the Raman peak (R).
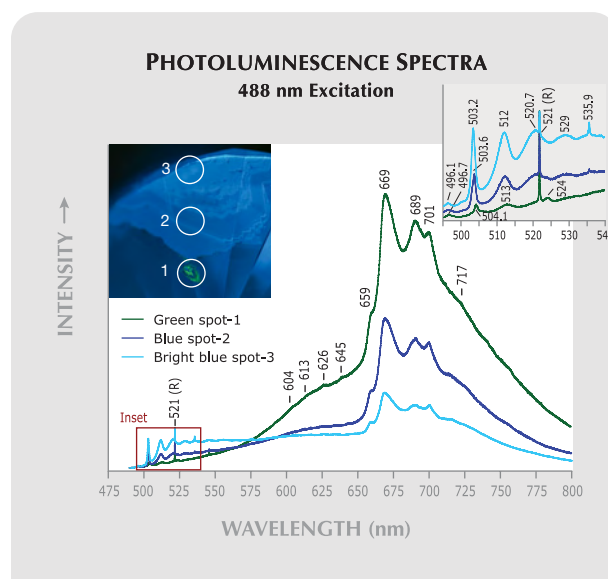
It contained the typical strong 669, 689, and 701 nm peaks, with accompanying 659 and 717 nm peaks. The 604 nm series was also present. The spectra also showed peaks at 496.7, 504.1, 513, and 524 nm (figure 16, inset).

The spectra from the blue-fluorescing regions had much lower overall luminescence in the 669, 689, and 701 nm peaks. Yet they had greater luminescence in the 495–575 nm region, where the spectra exhibited a 503.2 nm (H3) peak and its vibronic bands. No 524 nm peak was observed, but a 535.9 nm peak associated with (natural) radiation damage was present (again, see figure 16, inset).

DISCUSSION

Gemological Characteristics. The gemological characteristics of the HGBV diamonds in this study—etch features, color zoning, inclusions, and fluorescence reactions—were consistent with the diamonds described in Fritsch and Scarratt (1992, 1993) and more than 100 other small (0.03–0.10 ct) HGBV stones that were studied by Fritsch et al. (2007a).

Microscopic Characteristics. The internal features seen in HGBV diamonds are similar to those seen in pink diamonds from Argyle (e.g., Hofer, 1985; Fritsch et al., 2006). Some may have formed via geologic processes, such as dislocation- or cleavage-controlled etching (Lu et al., 2001; Fritsch et al., 2006), while others may be the result of the dissolution of crystal inclusions during processing and cleaning (Chapman, 1992). Indeed, the icicle-like acicular features and the cavities with radiating acicular points were quite similar in form to the inclusions with radiating acicular crystals (figure 7, left), so it is possible that mineral inclusions exposed at the surface of the diamond dissolved during cleaning.

Fluorescence. The yellow fluorescence of the samples to both long- and short-wave UV radiation may be related to their high H content, because it also occurs in H-rich diamonds of other colors—chameleon, gray-green, and orange (Eaton-Magaña et al., 2007).

When observed at shorter wavelengths using the DiamondView, the samples generally exhibited blue fluorescence. Caused by the N3 defect—groups of three nitrogen atoms and a vacancy along a {111} plane (e.g., Collins, 1999)—this is the most common fluorescence color in diamonds (Moses et al., 1997). The presence of N3 defects is not surprising, since the IR-active N

contents of the samples ranged up to 2700 ppm.

Some samples also exhibited yellowish green layers following the growth structures. Green fluorescence has typically been ascribed to the H3 center (Dyer and Matthews, 1958)—a vacancy plus an A-aggregate of nitrogen (Davies, 1972). However, Noble et al. (1998) and Iakoubovskii and Adriaenssens (2002) suggested that green fluorescence in HGBV diamonds might be related to nickel impurities. Spot PL analyses of one sample (figure 16) support this idea (see below).

Color Appearance and UV-Vis Characteristics. Because HGBV diamonds typically have very low color saturation and dark tone, no single hue or color description succinctly captures the color grades exhibited by this group. This has led both the trade and scientific literature to use a range of names to describe this material—for example, "hydrogen blue" or "Argyle blue" (Max, 2006), "violet" (Federman, 2003, 2007), and "blue-gray" (Iakoubovskii and Adriaenssens, 2002), "gray-blue" (Noble et al., 1998), and "blue-gray-violet" (De Weerdt and Van Royen, 2001).

One of the goals of this article was to refine the color terminology for HGBV diamonds. However, the range of color grades exhibited by the study samples further complicates the description of these diamonds based solely on color. We believe that calling them "gray to blue to violet," as in Fritsch et al. (2007a), or "HGBV" diamonds, remains the simplest solution, with the caveats that these color descriptions typically do not include unmodified blue or violet hues, and that none of the study samples (nor any of the diamonds offered at tender from 1993 to 2008) had bluish violet or violetish blue hues.

The apparent color of these diamonds results from the additive effect of the two broad absorption minima or transmission maxima—also known as transmission windows—in the blue and red regions (figure 10; see also Fritsch et al., 2007a). We found that the center positions of the transmission windows changed with hue: Samples with minima in the blue and red regions were violet-hued, whereas those with minima in the orange-to-yellow and blue-to-green regions were blue-hued (again, see figure 11B).

The apparent colors, however, depend not only on the positions of the transmission windows, but also on the windows' relative strengths (Fritsch et al., 2007a), which we investigated through a comparison of the ratios of the areas and depths of the features (figure 11C). As the ratio B_a/R_a increases, the

area (strength) of the blue window increases relative to the red window. For example, a value of 1 means that the absorptions in the blue and red regions were of equal strength, whereas a value of 2 means that the absorptions in the blue region were twice as strong as those in the red. Our data showed that HGBV diamonds with blue hues had higher B_a/R_a and B_d/R_d values than those with violet hues (figure 11C). The blue stones' absorption in the blue region was about twice as strong as in the red region. Violet stones had $B_a/R_a = 1.4–1.7$ and $B_d/R_d = 1.3–1.5$, so the area and depth of the absorption in the blue region still exceeded that of the absorption in the red region, but less than they did for the blue stones. It is unclear whether stones with $B_a/R_a \leq 1.4$ and $B_d/R_d \leq 1.3$ would be predominantly gray, blue, or violet, because there were samples with three different color grades in this area of the plot (figure 11C). In summary, when the absorption band in the blue region is broad, flat, and has an area twice as large as that of the red band, the stone appears blue; when it is relatively deep, with steep flanks, and an area ~1.5 times that of the red band, the stone appears violet.

The presence and relative strengths of the two transmission windows also explain why HGBV diamonds, particularly those with violet hues, have slightly different colors under different lighting conditions. Those with strong color saturation tend to appear slightly bluer under fluorescent lighting (stronger illumination in the blue region) and slightly more violet under incandescent lighting (stronger illumination in the red region). The violet-hued stones have transmission windows that are positioned wider apart than the blue-hued stones, so they are more sensitive to lighting conditions, especially those with different intensities in the blue and red wavelengths. The difference, however, is not great enough to consider them color-change diamonds.

Comparison with Type IIb Diamonds. Some HGBV color grades overlap those of electrically conductive type IIb diamonds (King et al., 1998), but there are usually subtle differences. This was demonstrated by Darley and King (2007) for another H-rich blue-gray diamond that was observed in GIA's New York laboratory. Even some HGBV diamonds that fall within the same color space as type IIb diamonds can be distinguished on the basis of these subtle color differences. For example, grayish blue and gray-blue HGBV diamonds tend to be slightly more violet than their type IIb equivalents, though they occupy the same color space and thus receive the
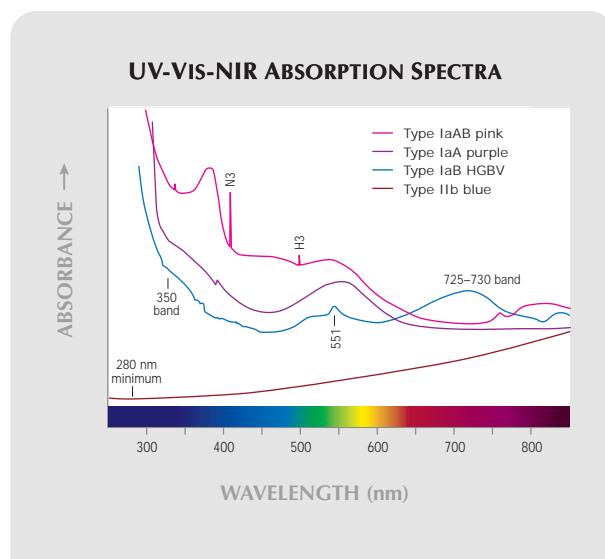

Figure 17. The UV-Vis-NIR spectra of HGBV diamonds differ greatly from the spectrum of a typical type IIb blue diamond; they are more similar to pink and purple diamonds. However, the 520–565 nm composite feature in HGBV diamonds is different from the 550–560 nm feature seen in some pink and purple diamonds, as shown by Gaussian spectral deconvolution (figure 3). The spectra were collected at ~77 K.

same color grades. In all cases, their UV-Vis-NIR spectra are very different, with most type IIb diamonds characterized by a simple spectrum consisting of an absorption minimum at 280 nm and a smooth, almost linear increase in absorption into the near-infrared region (figure 17). HGBV diamonds are also readily distinguished from type IIb diamonds by their nonconductivity and differences in UV fluorescence (e.g., Fritsch and Scarratt, 1992).

The quick separation of HGBV and type IIb diamonds is useful because HGBV diamonds are not known to be treated to enhance their color, whereas the color of type IIb diamonds may be improved via high-pressure, high-temperature (HPHT) treatment. In addition, synthetic blue diamonds typically fall into two categories—mixed types IIb+IIa or IIb+Ib—that also have different gemological properties from HGBVs (e.g., Shigley et al., 2004). The identification of a diamond as HGBV supports a natural origin and precludes special testing to determine whether HPHT treatment has occurred.

One unusual natural mixed type IIa+IIb diamond that was color graded light violet-gray has been documented (Reinitz and Moses, 1993). However, it was concluded that the color of this diamond was caused by the additive effect of separate pink type IIa and gray type IIb zones.

Comparison with Pink and Purple Diamonds. Previous work on HGBV diamonds (Noble et al., 1998) suggested that the 530–550 nm band had the same origin as the 550–560 nm broad band seen in some pink and purple diamonds (Collins, 1982; Moses et al., 2002; figure 17). In type IIa pink diamonds, the 550–560 nm broad band may result from nitrogen-vacancy defects (N-V centers), which also cause two strong absorptions at 575 and 637 nm (e.g., Scarratt, 1987; Fritsch et al., 2007b). The 520–565 nm composite band in HGBV diamonds clearly is not related to the N-V center, because neither the Gaussian decomposition nor the PL spectra showed major absorption features centered at 575 or 637 nm.

The defect responsible for the 550–560 nm broad band in type Ia pink and purple diamonds has not been established. It may be caused by plastic deformation, which has been observed in many pink and purple diamonds as anomalous double refraction (ADR) or high strain, and is typically, but not exclusively, confined to thin strain-related lamellae (Orlov 1977; De Weerdt and Van Royen, 2001; King et al., 2002; Moses et al., 2002; Titkov et al., 2008). HGBV diamonds do not show a high degree of ADR or strain, and their color is related to growth structures rather than deformation lamellae (figure 7); if the 550–560 nm absorption feature in pink and purple diamonds is the result of strong deformation, then the 520–565 nm absorption feature in HGBV diamonds does not have the same origin.

Roles of Hydrogen, Nitrogen, and Nickel.
Hydrogen. The relatively high hydrogen concentration in HGBV diamonds has been documented previously (e.g., Fritsch and Scarratt, 1989; Fritsch et al., 1991) and was recently reviewed and updated (Fritsch et al., 2007a). The H-related features usually seen in IR spectra include the 3107 cm^{-1} band and associated peaks at 6068, 5556, 4495, 4168, 2786, and 1405 cm^{-1}, which are likely the result of C-H vibration interacting with aggregated nitrogen. The peaks between 4705 and 3237 cm^{-1} may correspond to N-H vibration (Fritsch et al., 2007a). The origins of all the remaining IR peaks have not been determined thus far, but many have been observed in H-rich diamonds of various colors (Fritsch et al., 2007a).

The possible role of hydrogen in the coloration of H-rich diamonds, including HGBV diamonds, was first suggested by Fritsch and Scarratt (1989). Indeed, as illustrated by our Gaussian modeling of the UV-Vis spectra of HGBV diamonds, they may exhibit some of the same optical absorption bands as other H-rich diamonds. Peaks at 545 and 563 nm, possibly related to high hydrogen content, have been seen in brownish yellow or Cape yellow (e.g., De Weerdt and Van Royen, 2001) and chameleon (e.g., Hainschwang et al., 2005) diamonds. To date, however, it has not been shown definitively that IR-active hydrogen causes optically active absorption features, including the 545 and 563 nm bands (Fritsch et al., 2007a). Regardless, the presence of hydrogen probably is not the only factor involved in the coloration of H-rich diamonds, which exhibit a range of colors. It seems clear, though, that it may be an important prerequisite for the formation of the defects responsible for color in H-rich diamonds, as suggested by Iakoubovskii and Adriaenssens (2002) for HGBV diamonds.

Nitrogen. Five of the samples examined here exhibited high concentrations of IR-active nitrogen, present primarily as B aggregates (four-nitrogen defects), from 1350 to 2700 ppm. This confirms previous estimates that HGBV diamonds contain at least 500 ppm N (Fritsch and Scarratt, 1989). Nitrogen was found in HGBV diamonds not only as B aggregates, but also as low concentrations of N3 and N2 complexes (two types of three-nitrogen complexes; Iakoubovskii and Adriaenssens, 2002). Nitrogen and hydrogen concentrations are linked, such that they increase commensurately (e.g., Iakoubovskii and Adriaenssens, 2002; Rondeau et al., 2004), so it is not surprising that HGBV diamonds also have relatively high N contents.

Nickel. This element is an important factor in the PL spectra of HGBV diamonds. Numerous peaks attributed and tentatively attributed to Ni-N defects were seen (604, 645, 659, 669, 689, 694, 701, 788, and 794 [NE8] nm centers). In fact, in the present study the dominant luminescence features were stronger for the violet stones and also depended on the color saturation (figure 15). This indicates that the violet diamonds had higher concentrations of certain Ni-related defects than the blue diamonds.

While the PL spectra for the blue fluorescing areas did exhibit a peak at 503.2 nm (H3), the PL spectra for the yellowish green fluorescing area did not (figure 16). In addition, the yellowish green area had much stronger Ni-related peaks than the blue areas. This evidence supports the idea that yellowish green fluorescence in HGBV diamonds

is related to Ni-defects rather than the H3, as suggested by Iakoubovskii and Adriaenssens (2002) and Noble et al. (1998).

It is unknown what defects are responsible for most of the IR peaks from 10570 to 7490 cm^{-1}, but a peak at 10300 cm^{-1} has been seen in some synthetic Ni- and N-doped diamonds (Zaitsev, 2001). It remains to be tested whether these peaks, also seen in some other H-rich diamonds (Fritsch et al., 2007a), are related to H-, Ni-, and/or other defects.

One outstanding question is whether the Ni-related PL peaks in HGBV diamonds are optically active, as are all the Ni-related centers discovered thus far during EPR studies of synthetic diamonds (e.g., Yelisseyev and Kanda, 2007). One study of HPHT synthetic diamond grown in the Fe-Ni-C system (Yelisseyev et al., 2002) observed optical absorptions at 515.5, 518.0, 520.0, and 527.3 nm resulting from Ni-N complex defects that are possibly related to the 727 nm PL center (Lawson and Kanda, 1993; Yelisseyev and Nadolinny, 1995). These defects may contribute to the 520–530 nm component of the composite band seen in HGBV diamonds, especially since a 727 nm PL center was seen at the 514 and 633 nm excitation wavelengths. Alternatively, the 520–530 nm component could be related to the 524 nm band observed in the PL spectra. It is not clear whether this band might be related to the NE3, a Ni-related center at 523.3 nm.

A 732 nm optical center is also related to Ni-N complex defects (Lawson and Kanda, 1993), as observed in HPHT synthetic diamonds (Yelisseyev et al., 2002). Previous observations of HGBV diamonds (Noble et al., 1998) noted that it is impossible to speculate on the origin of the broad band centered at 720–730 nm because of the absence of sharp lines or structures. However, our data indicate that this absorption is stronger for violet-hued HGBV diamonds with more saturated color (figure 10). Further EPR studies of HGBV diamonds with a range of color grades are necessary to investigate the origins of possible Ni-related optical features more fully.

Higher Ni concentrations in diamond may also correspond to higher N and H concentrations (e.g., Lang et al., 2004). It follows that when both Ni and N are present more Ni-N defects could form, for example, in HGBV diamonds. Indeed, Noble et al. (1998) suggested that Ni-N interactions might influence the color of these diamonds. Yet Ni is also present, for example, in chameleon diamonds (Hainschwang et al., 2005) and some natural-color green-yellow diamonds (Wang et al., 2007); thus,

Figure 18. This rare 1.41 ct Fancy Dark gray-violet octagonal-cut HGBV diamond, named "Ocean Seer," was sold at the 2008 Argyle pink diamond tender. Courtesy of Argyle Diamonds.

the colors of these diamonds do not depend simply on the presence of Ni. Perhaps the variety of colors could result from different Ni defects. For example, one of the EPR centers observed by Noble et al. (1998), proposed as Ni$_s^-$ with N$^+$ in a fourth nearest-neighbor position, was seen only in HGBV diamonds in their study and not in other diamond colors from the Argyle mine. High H and N concentrations may be required for *different* Ni and Ni-N defects to form in HGBV and other H-rich diamonds that ultimately give rise to different apparent colors. A slight variation in the relative concentrations of specific defects could be responsible for the color variations in HGBV diamonds.

CONCLUSIONS

One of the more unusual varieties of fancy-color diamonds is that represented by type IaB hydrogen-rich "gray to blue to violet," or "HGBV," diamonds (see, e.g., figure 18), which to date are only known from the Argyle mine in Australia. This study of HGBV diamonds revealed systematic relationships between their spectroscopic properties and color grades. It also confirmed previous work documenting numerous H-related IR peaks in HGBV diamonds. Many H-related peaks were stronger in the violet- than the blue-hued samples, indicating that violet-hued stones may have higher H concentrations. We also confirmed and expanded on work showing that nick-

el-related defects are observed in the PL spectra of HGBV diamonds. Indeed, the luminescence of the Ni-related peaks was stronger in the violet- than the blue-hued samples, suggesting a higher concentration of these Ni-defects in the violet-hued stones. In addition, we showed that yellowish green fluorescence in HGBV diamonds is correlated with PL-active Ni-defects.

The color of HGBV diamonds is the additive effect of two transmission windows in the blue and red areas of the visible region. The positions and strengths of these windows directly affect apparent color. Spectral deconvolution showed that the composite absorption feature centered at 520–565 nm could be a combination of peaks observed in other H-rich diamonds (545 and 563 nm) and 551 and ~520–530 nm peaks. This finding underscores their close relationship to other H-rich diamonds. Overall, the gemological and spectroscopic characteristics of HGBV diamonds separate them from other types of diamonds of similar color that may be treated or even synthetic.

ABOUT THE AUTHORS
Dr. van der Bogert is a senior research scientist at Westfaelische Wilhelms University in Muenster, Germany. At the time this article was accepted, Mr. Smith was vice president and chief gemologist at the American Gemological Laboratories in New York. Mr. Hainschwang is director of the Gemlab Laboratory for Gemstone Analysis and Reports in Liechtenstein. Mr. McClure is director of Identification Services at the GIA Laboratory in Carlsbad, California. Both Dr. van der Bogert and Mr. Smith performed research for this article while employed at the GIA Laboratory in New York, and Mr. Hainschwang did so with the former GIA GemTech Laboratory in Geneva, Switzerland.

REFERENCES

Argyle Diamonds (1993–2008) *Pink Diamond Tender* [annual catalog]. West Perth, Australia.

Bokii G.B., Bezrukov G.N., Klyuev Yu.A., Naletov A.M., Nepsha V.I. (1986) *Natural and Synthetic Diamonds*. Nauka, Moscow (in Russian).

Boyd S.R., Kiflawi I., Woods G.S. (1995) Infrared absorption by the B nitrogen aggregation in diamond. *Philosophical Magazine B*, Vol. 72, No. 3, pp. 351–361.

Burns R.G. (1993) *Mineralogical Applications of Crystal Field Theory*. Cambridge University Press, Cambridge, UK, 575 pp.

Chapman J. (1992) Letters: Hollow hexagonal columns in diamond not etch pits. *G&G*, Vol. 28, No. 1, p. 73.

Collins A.T. (1982) Colour centers in diamond. *Journal of Gemmology*, Vol. 18, No. 1, pp. 37–75.

Collins A.T. (1999) Things we still don't know about optical centers in diamond. *Diamond and Related Materials*, Vol. 8, No. 8–9, pp. 1455–1462.

Darley J., King J.M. (2007) Lab Notes: Natural color hydrogen-rich blue-gray diamond. *G&G*, Vol. 43, No. 2, pp. 155–156.

Davies G. (1972) The effect of nitrogen impurity on the annealing of radiation damage in diamond. *Journal of Physics C: Solid State Physics*, Vol. 5, No. 17, pp. 2534–2542.

De Weerdt F., Van Royen J. (2001) Defects in coloured natural diamonds. *Diamond and Related Materials*, Vol. 10, No. 3–7, pp. 474–479.

Dyer H.B., Matthews I.G. (1958) The fluorescence of diamond. *Proceedings of the Royal Society of London A*, Vol. 243, No. 1234, pp. 320–335.

Eaton-Magaña S., Post J.E., Heaney P.J., Walters R.A., Breeding C.M., Butler J.E. (2007) Fluorescence spectra of colored diamonds using a rapid, mobile spectrometer. *G&G*, Vol. 43, No. 4, pp. 332–351.

Federman D. (2003) Gem Profile—Purple and violet diamonds: Kissing cousins. *Modern Jeweler*, Vol. 102, No. 9, pp. 47–48.

Federman D. (2007) Gem Profile—Violet diamond. *Modern Jeweler*, www.modernjeweler.com/web/online/Diamond-Gem-Profiles/Violet-Diamond/2$284 [accessed Oct. 27, 2008].

Fritsch E., Scarratt K. (1989) Optical properties of some natural diamonds with high hydrogen content. In A. Feldman and S. Holly, Eds., *Diamond Optics II*, Society for Photo-optical Instrumentation Engineers, Bellingham, WA, pp. 201–206.

Fritsch E., Scarratt K. (1992) Natural-color nonconductive gray-to-blue diamonds. *G&G*, Vol. 28, No. 1, pp. 35–42.

Fritsch E., Scarratt K. (1993) Gemmological properties of type Ia diamonds with an unusually high hydrogen content. *Journal of Gemmology*, Vol. 23, No. 8, pp. 451–460.

Fritsch E., Scarratt K., Collins A.T. (1991) Optical properties of diamonds with an unusually high hydrogen content. In R. Messier, J.T. Glass, J.E. Butler, and R. Roy, Eds., *Materials Research Society International Conference Proceedings*, Second International Conference on New Diamond Science and Technology, Washington, DC, Sept. 23–27, Materials Research Society, Pittsburgh, PA, pp. 671–676.

Fritsch E., Rondeau B., Notari F. (2006) Cleavage resistance of plastically deformed natural diamonds revealed by dissolved planar features. *Diamond and Related Materials*, Vol. 15, No. 9, pp. 1310–1313.

Fritsch E., Hainschwang T., Massi L., Rondeau B. (2007a) Hydrogen-related optical centers in natural diamond: An update. *New Diamond and Frontier Carbon Technology*, Vol. 17, No. 2, pp. 63–89.

Fritsch E., Rondeau B., Hainschwang T., Quellier M.-H. (2007b) A contribution to the understanding of pink color in diamond: The unique, historical "Grand Condé." *Diamond and Related Materials*, Vol. 16, No. 8, pp. 1471–1474.

Gaffey M.J., Bell J.F., Brown R.H., Burbine T.H., Piatek J.L., Reed K.L., Chaky D.A. (1993) Mineralogical variations within the S-type asteroid class. *Icarus*, Vol. 106, No. 2, pp. 573–602.

Hainschwang T., Simic D., Fritsch E., Deljanin B., Woodring S., Del Re N. (2005) A gemological study of a collection of chameleon diamonds. *G&G*, Vol. 41, No. 1, pp. 20–35.

Hofer S.C. (1985) Pink diamonds from Australia. *G&G*, Vol. 21, No. 3, pp. 147–155.

Iakoubovskii K., Adriaenssens G.J. (2002) Optical characterization of Argyle diamonds. *Diamond and Related Materials*, Vol. 11, No. 1, pp. 125–131.

Kiflawi I., Mayer A.E., Spear P.M., Van Wyck J.A., Woods G.S. (1994) Infrared absorption by the single nitrogen and A defect centres in diamond. *Philosophical Magazine B*, Vol. 69, No. 6, pp. 1141–1147.

King J.M., Moses T.M., Shigley J.E., Liu Y. (1994) Color grading of colored diamonds in the GIA Gem Trade Laboratory. *G&G*, Vol. 30, No. 4, pp. 220–242.

King J.M., Moses T.M., Shigley J.E., Welbourn C.M., Lawson S.C., Cooper M. (1998) Characterizing natural-color type IIb blue diamonds. *G&G*, Vol. 34, No. 4, pp. 246–268.

King J.M., Shigley J.E., Guhin S.S., Gelb T.H., Hall M. (2002) Characterization and grading of natural-color pink diamonds. *G&G*, Vol. 38, No. 2, pp. 128–147.

Lang A.R., Yelisseyev A.P., Pokhilenko N.P., Steeds J.W., Wotherspoon A. (2004) Is dispersed nickel in natural diamonds associated with cuboid growth sectors in diamonds that exhibit a history of mixed-habit growth? *Journal of Crystal Growth*, Vol. 263, pp. 575–589.

Lawson S.C., Kanda H. (1993) An annealing study of nickel point defects in high-pressure synthetic diamond. *Journal of Applied Physics*, Vol. 73, No. 8, pp. 3967–3973.

Lu T., Shigley J.E., Koivula J.I., Reinitz I.M. (2001) Observation of etch channels in several natural diamonds. *Diamond and Related Materials*, Vol. 10, No. 1, pp. 68–75.

Massi L. (2006) Etudes des Défants dans les Diamants Bruns et les Diamants Riches en Hydrogène. PhD thesis, University of Nantes, France, 372 pp. (in French).

Max D. (2006) One in a million—The Rio Tinto Diamonds Argyle pink diamond tender report. *Idex Magazine*, No. 199, November 13, pp. 75–79, www.idexonline.com/portal_FullMazalUbracha.asp?id=26439 [accessed Oct. 27, 2008].

Moses T.M., Reinitz I.M., Johnson M.L., King J.M., Shigley J.E. (1997) A contribution to understanding the effect of blue fluorescence on the appearance of diamonds. *G&G*, Vol. 33, No. 4, pp. 244–259.

Moses T.M., King J.M., Wang W., Shigley J.E. (2002) A highly unusual 7.34 carat vivid purple diamond. *Journal of Gemmology*, Vol. 28, No. 1, pp. 7–12.

Nadolinny V., Yelisseyev A. (1994) New paramagnetic centers containing nickel ions in diamond. *Diamond and Related Materials*, Vol. 3, No. 1–2, pp. 17–21.

Noble C.J., Pawlik Th., Spaeth J.-M. (1998) Electron paramagnetic resonance investigations of nickel defects in natural diamonds. *Journal of Physics: Condensed Matter*, Vol. 10, pp. 11781–11793.

Orlov Y.L. (1977) *The Mineralogy of Diamond*. J. Wiley & Sons, New York.

Reinitz I.M., Moses T.M. (1993) Gem Trade Lab Notes: Light violet-gray diamond. *G&G*, Vol. 29, No. 3, p. 199.

Rio Tinto (2009) Rio Tinto tenders a rare offering of blue diamonds. www.riotintodiamonds.com/ENG/media/media_releases_1144.asp [accessed Mar. 9, 2009]

Rondeau B., Fritsch E., Guiraud M., Chalain J.-P., Notari F. (2004) Three historically "asteriated" hydrogen-rich diamonds: Growth history and sector-dependent impurity incorporation. *Diamond and Related Materials*, Vol. 13, pp. 1658–1673.

Scarratt K. (1987) Notes from the laboratory – 10. *Journal of Gemmology*, Vol. 20, No. 6, pp. 356–361.

Shigley J.E., Chapman J., Ellison R.K. (2001) Discovery and mining of the Argyle diamond deposit, Australia. *G&G*, Vol. 37, No. 1, pp. 26–41.

Shigley J.E., McClure S.F., Breeding C.M., Shen A.H., Muhlmeister S.M. (2004) Lab-grown colored diamonds from Chatham Created Gems. *G&G*, Vol. 40, No. 2, pp. 128–145.

Titkov S.V., Shigley J.E., Breeding C.M., Mineeva R.M., Zudin N.G., Sergeev A.M. (2008) Natural-color purple diamonds from Siberia. *G&G*, Vol. 44, No. 1, pp. 56–64.

Wang W., Hall M., Breeding C.M. (2007) Natural type Ia diamond with green-yellow color due to Ni-related defects. *Gems & Gemology*, Vol. 33, No. 3, pp. 240–243.

Welbourn C.M., Cooper M., Spear P.M. (1996) De Beers natural versus synthetic diamond verification instruments. *G&G*, Vol. 32, No. 3, pp. 156–169.

Woods G.S., Collins A.T. (1983) Infrared absorption spectra of hydrogen complexes in type I diamond. *Journal of Physics and Chemistry of Solids*, Vol. 44, No. 5, pp. 471–475.

Yelisseyev A., Babich Yu., Nadolinny V., Fisher D., Feigelson B. (2002) Spectroscopic study of HPHT diamonds, as grown at 1500°C. *Diamond and Related Materials*, Vol. 11, No. 1, pp. 22–37.

Yelisseyev A., Kanda H. (2007) Optical centers related to 3d transition metals in diamond. *New Diamond and Frontier Carbon Technology*, Vol. 17, No. 3, pp. 127–178.

Yelisseyev A., Nadolinny V. (1995) Photoinduced absorption lines related to nickel impurity in annealed synthetic diamonds. *Diamond and Related Materials*, Vol. 4, No. 3, pp. 177–185.

Zaitsev A.M. (2001) *Optical Properties of Diamond: A Data Handbook*. Springer-Verlag, Berlin, 502 pp.